

First-principles study of atomic structure and electronic properties of Si and F doped anatase TiO₂

HONGPING LI^{1*}, LIN CHEN¹, SHUAI LIU¹, CHANGSHENG LI¹, JIAN MENG²,
ZHONGCHANG WANG³

¹Institute for Advanced Materials, School of Materials Science and Engineering, Jiangsu University, Zhenjiang, 212013, P. R. China

²State Key Laboratory of Rare Earth Resources Utilization, Changchun Institute of Applied Chemistry, Chinese Academy of Sciences, Changchun, 130022, P. R. China

³Advanced Institute for Materials Research, Tohoku University, 2-1-1 Katahira, Aoba-ku, Sendai 980-8577, Japan

Chemical doping represents one of the most effective ways in engineering electronic structures of anatase TiO₂ for practical applications. Here, we investigate formation energies, geometrical structures, and electronic properties of Si-, F-doped and Si/F co-doped anatase TiO₂ by using spin-polarized density functional theory calculation. We find that the co-doped TiO₂ is thermodynamically more favorable than the Si- and F-doped TiO₂. Structural analysis shows that atomic impurity varies crystal constants slightly. Moreover, all the three doped systems show a pronounced narrowing of band gap by 0.33 eV for the F-doped TiO₂, 0.17 eV for the Si-doped TiO₂, and 0.28 eV for the Si/F-co-doped TiO₂, which could account for the experimentally observed redshift of optical absorption edge. Our calculations suggest that the Si/F-co-doping represents an effective way in tailoring electronic structure and optical properties of anatase TiO₂.

Keywords: anatase TiO₂; Si/F co-doping; first-principles; electronic properties

© Wrocław University of Technology.

1. Introduction

As a chemically stable, nontoxic, highly efficient, and relatively inexpensive photocatalyst [1, 2], TiO₂ has aroused extensive attention recently owing to its potential use in water and air purification. However, its photoreaction efficiency is severely limited due to its large intrinsic band gap (3.23 eV for anatase TiO₂). TiO₂ is only capable of absorbing the ultraviolet portion of the solar spectrum [3, 4]. It is, thus, necessary to enhance its optical absorption in the visible range to efficiently utilize a wider range of solar light. Since Sato reported that nitrogen doping in TiO₂ can result in the visible-light photocatalytic activity [5], a huge number of chemical modifications have been conducted to investigate the doping effect of TiO₂ both theoretically and experimentally [6–10]. However,

the photocatalytic efficiency of the N-doped TiO₂ can only be improved in a limited way due to the strongly localized N p states at the top of the valence band [11]. It has been recognized that the donor-acceptor co-doping at Ti and O sites could reduce recombination centers, which can effectively improve migration efficiency of charge carriers and enhance photocatalytic activity [12–16].

Since Yang et al. [17] found that F can largely stabilize the reactive (001) facets of TiO₂ nanoparticles, much effort has been devoted to the study of the F-doped TiO₂. Zhou et al. [18] further investigated the C–F co-doped anatase TiO₂ (001) surfaces, and found that photocatalytic activity of TiO₂ can be enhanced dramatically. In addition, Oh et al. [19] reported that doping TiO₂ with a small amount of Si could improve its photocatalytic activity. Ozaki et al. [20] suggested that the substitution of Ti by Si may promote photocatalytic activity by extending optical absorption to longer

*E-mail: hpli@mail.ujs.edu.cn

wavelength. Yang *et al.* [21] studied electronic properties of the substitutional Si-doped TiO₂, and found that the band gap can be narrowed by Si doping. Recently, experimental studies have shown that the co-doping with nonmetal materials can be more effective to improve the photocatalytic activity of TiO₂ [22, 23]. To modify the valence band edge (i.e. p-type doping), one may choose two nonmetal atoms with a different p orbital energy from that of O [24] to dope TiO₂, which may represent a prominent method to enhance the photocatalytic activity of TiO₂. For instance, Ozaki *et al.* [25] prepared Si/N-codoped anatase TiO₂ and found that its properties can be significantly improved by optimizing the Si/Ti ratio. To obtain enhanced photocatalytic activities of anatase TiO₂ [26], we have conducted first-principles calculations to investigate the effect of Si/F-co-doping on atomic structures and electronic properties of anatase TiO₂. To uncover the effect of Si or F impurity on electronic properties, we also considered the Si- and F-doped anatase TiO₂ for comparison. Our results show that the band gap is remarkably narrowed for all the doped systems, which should be beneficial for the optical absorption.

2. Computational details

First-principles plane-wave pseudopotential calculations based on the density functional theory (DFT) [27] was performed using the Cambridge Sequential Total Energy Package Code (CASTEP) [28]. The geometry optimization was carried out by the Broyden-Fletcher-Goldfrab-Shanno (BFGS) method. The plane wave cut-off energy was chosen to be 400 eV for all calculations. The generalized gradient approximation (GGA) within the Perdew-Burke-Ernzerhof (PBE) scheme [29] was employed to describe the exchange-correlation functional. The Monkhorst-Pack k-mesh was set to be $5 \times 5 \times 4$. Electron-ion interactions were described by the ultrasoft pseudopotentials with the valence electron configurations $3s^2 3p^6 3d^2 4s^2$, $3s^2 3p^2$, $2s^2 2p^5$ and $2s^2 2p^4$ for Ti, Si, F and O, respectively. Self-consistence was achieved once the total energy was converged to less than 1.0×10^{-5} eV and the maximum force fell below 0.03 eV/Å.

To properly describe the strong electron correlation in 3d transition metal oxide, the GGA plus on-site repulsion U method (GGA + U) was employed [30, 31]. A series of U values was tested for the Ti 3d orbitals. The band gap for pure TiO₂ was calculated to be 2.95 eV when the U was set to 7.0 eV, in agreement with previous GGA + U theoretical results [24, 32]. We, therefore, selected the U values as 7.0 eV to address the Ti 3d orbital electrons.

3. Results and discussion

Anatase TiO₂ has a body-centered tetragonal crystal structure with I₄₁/amd space group [33], and there are four Ti atoms and eight O atoms in each unit cell. A supercell of $2 \times 2 \times 1$ anatase TiO₂ (Fig. 1a) has been constructed to calculate its electronic properties. For the F-doped (Si-doped) model, an O (Ti) atom is replaced by a F (Si) atom and the doping concentration is 2.08 at.%. For the F/Si-co-doped anatase TiO₂, an O atom is substituted by a F atom, while a Ti atom is substituted by a Si atom (Fig. 1b). The doping concentration is 4.17 at.%. To investigate how the distance of doped Si and F affects the crystal structures and electronic properties, we have considered three typical co-doping models: (i) a Ti atom is replaced by a Si, while its nearest-neighbor O is substituted by a F (Fig. 1b). The Si and F distance is the shortest in this supercell (named Si/F-I), (ii) the substituted Si and F atoms are 3.847 Å far apart (Fig. 1c, named Si/F-II), and (iii) a much longer distance (5.477 Å) between Si and F atoms is adopted (Fig. 1d, named Si/F-III).

To determine a relative stability of the doped systems, we conducted calculations on formation energy, a relevant physical quantity to evaluate the relative difficulty in incorporating a dopant into a host lattice, according to the formula below [34]:

$$E_{f(F)} = E_{(F)} - E_{(pure)} - \mu_F + \mu_O \quad (1)$$

$$E_{f(Si)} = E_{(Si)} - E_{(pure)} - \mu_{Si} + \mu_{Ti} \quad (2)$$

$$E_{f(Si/F)} = E_{(Si/F)} - E_{(pure)} - \mu_F - \mu_{Si} + \mu_{Ti} + \mu_O \quad (3)$$

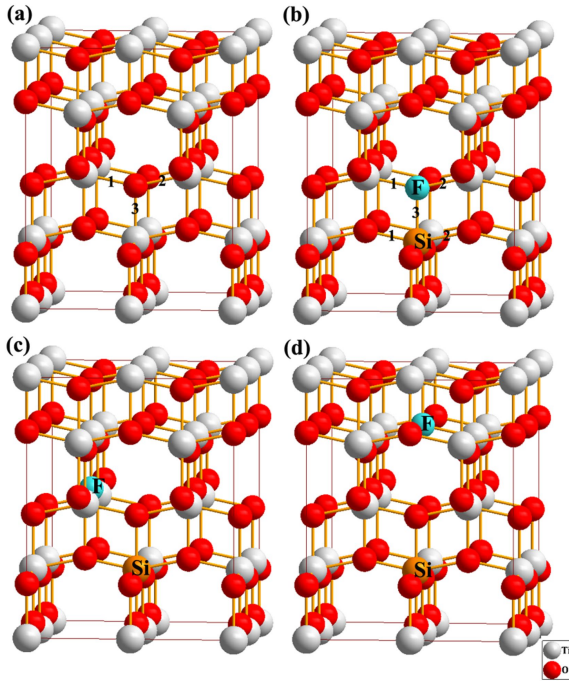


Fig. 1. Side view of the $2 \times 2 \times 1$ supercells for the (a) pure and (b-d) three models of the Si/F-co-doped TiO₂. In the Si/F-co-doped system, an F atom is substituted by an O atom, while a Si atom is substituted by a Ti atom.

where $E_{f(F)}$, $E_{f(Si)}$, $E_{f(Si/F)}$ and $E_{(pure)}$ are calculated energies of F-doped, Si-doped and Si/F-co-doped TiO₂ supercells, and the μ_F and μ_{Si} are chemical potentials of F and Si impurity, respectively. The formation energy depends on the growth condition and varies from Ti- to O-rich. For TiO₂, μ_O and μ_{Ti} satisfy the relationship $\mu_{Ti} + 2\mu_O = \mu(TiO_2)$. Under O-rich condition, μ_O is determined by energy of an O₂ molecule and μ_{Ti} is determined from the formula. On the other hand, under Ti-rich condition, μ_{Ti} is the energy of a Ti atom in bulk Ti and μ_O is calculated by the formula. Table 1 lists the calculated formation energies. From the Table, one can notice that (1) F-doped TiO₂ is more thermodynamically stable under Ti-rich condition; (2) Ti is readily to be substituted by Si under both the Ti- and O-rich conditions. Moreover, the substitution is more preferred under O-rich condition; (3) all the three Si/F-co-doped configurations are stable irrespective of the Ti-rich and O-rich conditions, i.e. the incorporation of F promotes the

Si doping under both Ti-rich and O-rich conditions, which indicates that F can enhance Si concentration in Si-doped TiO₂. We further notice that the Si/F-I configuration is the most stable one, although all the three co-doped configurations are also thermodynamically stable, indicating that the Si/F-I model is more favorable. We will, hence, present the results of Si/F-I in the following discussion.

Table 1. Formation energies E_f (eV) for the F-doped, Si-doped, and F/Si-co-doped anatase TiO₂.

		Ti-rich	O-rich
$E_{f(F)}$	F-doped	-0.99	-0.05
$E_{f(Si)}$	Si-doped	-5.88	-7.76
	Si/F-I	-7.42	-8.37
$E_{f(Si/F)}$	Si/F-II	-6.88	-7.83
	Si/F-III	-6.95	-7.89

Table 2 lists optimized structural parameters for pure and doped $2 \times 2 \times 1$ anatase TiO₂ supercell. The calculated lattice constants for pure TiO₂ supercell are $a = b = 7.601 \text{ \AA}$ and $c = 9.703 \text{ \AA}$, consistent with previous calculations, validating the application of our models and calculational method. In spite of the fact that the structural parameters are slightly overestimated (the experimental parameters are $a = b = 7.570 \text{ \AA}$ and $c = 9.514 \text{ \AA}$) [35] due to the well-known drawback of DFT, the results for electronic properties are not affected. In comparison to pure TiO₂, the doped case shows a slightly extended in-plane lattice constant after the substitution of O by F, which is attributed to the larger ionic radius of F. As a result, the Ti-F bonds (bond 1 and bond 2) are longer than the Ti-O bonds (Table 2), suggesting that the Ti-F bonds have a weaker covalency than the Ti-O. This is also verified by the charge density (Fig. 2a), in which overlapping of Ti 3d orbital with F 2p orbital is less pronounced than that of Ti 3d with O 2p orbitals. Meanwhile, the weaker Ti-F covalent bonds lead to a slight expansion of the crystal structure, and its volume is slightly increased by 0.39 % in the F-doped anatase TiO₂. In contrast, all lattice parameters in the Si-doped model are

decreased substantially with the volume constriction (560.606 \AA^3 for the pure TiO_2 and 552.180 \AA^3 for the Si-doped TiO_2). Accordingly, the Si–O bonds are also shrunk by $\sim 0.101 \text{ \AA}$. As seen in Fig. 2b, three O atoms nearest to Si are overlapped, indicating that the Si and O atoms are strongly covalent bonded. In F/Si-co-doped model, the in-plane lattice parameters are decreased, while the c axis is extended by $\sim 0.043 \text{ \AA}$ as compared to the pure TiO_2 . It is noteworthy that the Si–F bond is significantly extended, resulting in a slight structural distortion. Further, the F atom is pushed far away from the Si atom, as seen in the contour plot of charge density (Fig. 2c). Moreover, in the co-doped case, the Ti–F bonds are somewhat extended in comparison to the Ti–O bonds in pure TiO_2 , yet are shorter than the Ti–F bonds in the F-doped case. The Si–O bonds are shorter than those in Si-doped case and the Ti–O bonds in pure TiO_2 .

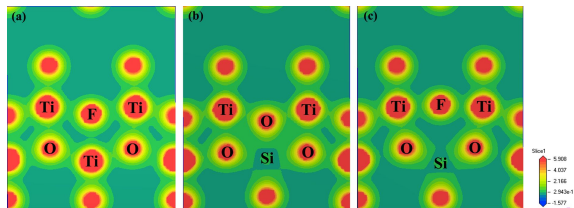


Fig. 2. Contour plots of charge densities for (a) F-doped TiO_2 , (b) Si-doped TiO_2 , and (c) Si/F-co-doped TiO_2 viewed on the (001) plane.

Fig. 3 shows the band structure of pure and three doped TiO_2 . The calculated band gap of pure anatase TiO_2 is 2.95 eV (Fig. 3a), which is consistent with the reported results [24, 32]. However, the Fermi level in the F-doped case shifts from the top of valence band to the bottom of conduction band, which is a typical characteristic of the n-type doping. Especially, the band gap is reduced to 2.62 eV (Fig. 3b) by F doping. Furthermore, there appear isolated impurity states around the Fermi level (E_F), i.e. the electron transfer from the fully occupied states to conduction band minimum (CBM) can reduce the photon transition energy significantly, which should enhance the red shift in the fundamental absorption edge of anatase TiO_2 . In the Si-doped TiO_2 , no impure states are induced by the Si doping, but

its band gap is decreased from 2.95 eV to 2.78 eV , rendering the electronic transfer from valence band maximum (VBM) to CBM easier. Moreover, there is no spin splitting in the Si-doped TiO_2 due to the identical feature of the spin-up and spin-down channels (Fig. 3c). The band structure of the Si/F-co-doped system is quite similar to that of F-doped case (Fig. 3d), showing isolated impurity states between the CBM and VBM. The band gap of the co-doped TiO_2 is reduced to 2.67 eV , smaller than that of the pure TiO_2 . Compared with the band structures of F-doped TiO_2 , the isolated impurity states do not overlap E_F and the energy between the impurity states and CBM increases from 0.58 eV to 1.24 eV .

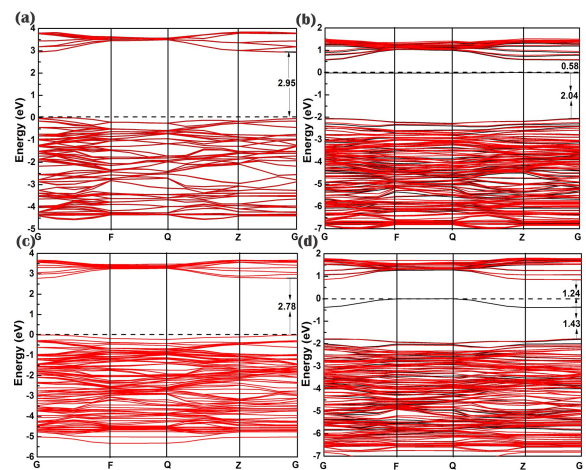


Fig. 3. Band structure diagrams for the pure and doped anatase TiO_2 : (a) pure TiO_2 , (b) F-doped TiO_2 , (c) Si-doped TiO_2 , and (d) Si/F-co-doped TiO_2 . The black lines represent the spin-up bands, while the red lines represent the spin-down bands. The dashed and horizontal lines define the Fermi level.

The total density of states (TDOS) and projected density of states (PDOS) for the pure and three doped TiO_2 are shown in Fig. 4. For the pure TiO_2 (Fig. 4a), the top of VB is mainly composed of O 2p states and the bottom of CB band is dominated by Ti 3d states. The E_F in F-doped case is shifted to higher energy as compared to that in the pure case (Fig. 4b). Some F 2p states are hybridized with Ti 3d states in the VB, while other F 2p states are localized on the VBM

Table 2. The optimized structural parameters for the pure and the doped $2 \times 2 \times 1$ TiO₂ supercells. In the F/Si-codoped configuration, the numbers with an asterisk in the Bond₁ and Bond₂ columns represent the Ti–F bond length, while those with a pound represent the Si–O bond length.

Configurations	a (Å)	b (Å)	c (Å)	c/a	Bond ₁	Bond ₂	Bond ₃	V (Å ³)
TiO ₂	7.601	7.601	9.703	1.277	1.947	1.947	2.004	560.606
F-doped	7.644	7.635	9.643	1.262	2.042	2.042	2.243	562.775
Si-doped	7.560	7.560	9.662	1.278	1.846	1.846	1.782	552.180
F/Si-codoped	7.566	7.572	9.746	1.288	$\frac{1.955^*}{1.730^\#}$	$\frac{1.955^*}{1.730^\#}$	2.799	558.361

top as acceptor level. Moreover, there appears asymmetric density of states, which arise from the Ti 3d states and O 2p states around E_F . These states may enhance the electron excitation from the VB to the CB by serving as a bridge by the visible-light absorption, which is responsible for red shifts in the absorption edge of TiO₂. Fig. 4c shows the TDOS and PDOS of the Si-doped TiO₂, which are almost identical to those of pure TiO₂ (Fig. 4a) except the reduced band gap. Some Si 3p states are hybridized with O 2p states in the VB band. In addition, there are also asymmetric DOSs in the Si/F-co-doped TiO₂ case, which are contributed by Ti 3d states and O 2p states around E_F (Fig. 4d), as seen in the case of the F-doped TiO₂. Likewise, the electronic states can also act as a bridge for electron excitation from VB to CB. One, hence, expects that optical properties may be improved in the Si/F-co-doped anatase TiO₂.

4. Conclusions

We have conducted a first-principles study of atomic structures and electronic properties of F-doped, Si-doped and Si/F-co-doped anatase TiO₂, aimed at engineering its electronic structure. The dopant formation energy calculations indicate that the Si/F-co-doped case is more thermodynamically preferred than the F- and Si-doped cases. The incorporation of F promotes the Si doping at both Ti-rich and O-rich conditions. Structural analysis demonstrates that atomic impurity imposes a little effect on crystal constants. The Ti–F covalent bonds are weaker than the Ti–O bonds because

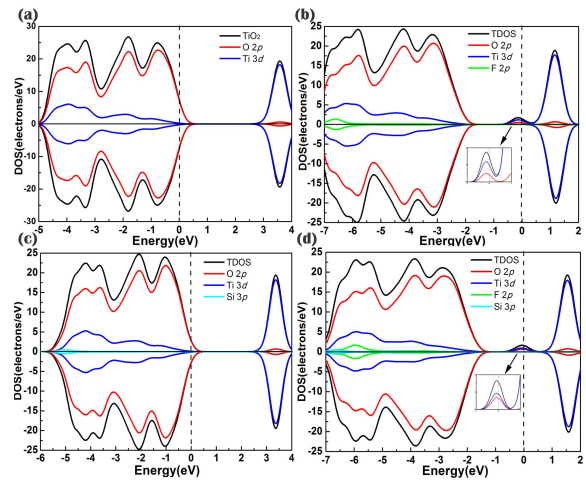


Fig. 4. Total DOS and PDOS for (a) pure TiO₂, (b) F-doped TiO₂, (c) Si-doped TiO₂, and (d) Si/F-co-doped TiO₂. The Fermi level is aligned to zero and indicated by a vertical dashed line.

they are longer, yet the Si–O bonds are shorter than the Ti–O ones. Moreover, the F-, Si-, and Si/F-co-doping narrow the band gap by 0.33, 0.17 and 0.28 eV, respectively. The decrease in electron transition energy from the VBM to CBM may be responsible for the visible-light optical absorption. Our calculations suggests that Si/F-co-doping is a useful way to tailor electronic structure and improve the optical properties of anatase TiO₂.

Acknowledgements

This work was supported by the National Natural Science Foundation of China under Grant No. 21301075, 51302112, the Specialized Research Fund for Doctoral Program of Higher Education (Grant No. 20133227120003), and Research Foundation for Advanced Talents of Jiangsu University (Grant No. 12JDG096). Z.W. thanks financial supports from

Grant-in-Aid for Young Scientists (A) (Grant No. 24686069), NSFC (Grant No. 11332013), JSPS and CAS under the Japan-China Scientific Cooperation Program, Murata Science Foundation, and Shorai Foundation for Science and Technology.

References

- [1] LINSEBIGLER A.L., LU G.Q., YATES J.T., *Chem. Rev.*, 95 (1995), 735.
- [2] FUJISHIMA A., HONDA K., *Nature*, 238 (1972), 37.
- [3] GRATZEL M., *Nature*, 414 (2001), 338.
- [4] ASAHI R., MORIKAWA T., OHWAKI T., AOKI K., TAGA Y., *Science*, 293 (2001), 269.
- [5] SATO S., *Phys. Chem. Lett.*, 123 (1986), 126.
- [6] ZHOU P., YU J.G., WANG Y.X., *Appl. Catal. B-Environ.*, 142 (2013), 45.
- [7] YU J.G., XIANG Q.J., ZHOU M.H., *Appl. Catal. B-Environ.*, 90 (2009), 595.
- [8] CHI B., ZHAO L., JIN T., *J. Phys. Chem. C*, 111 (2007), 6189.
- [9] YU J.G., ZHOU P., LI Q., *Phys. Chem. Chem. Phys.*, 15 (2013), 12040.
- [10] LIN Z., ORLOV A., LAMBERT R.M., PAYNE M.C., *J. Chem. Phys. B*, 109 (2005), 20948.
- [11] VALENTIN C.D., PACCHIONI G., SELLONI A., *Phys. Rev. B*, 70 (2004), 085116.
- [12] GAI Y., LI J., LI S.S., XIA J.B., WEI S.H., *Phys. Rev. Lett.*, 102 (2009), 036402.
- [13] XING M.Y., ZHANG J.L., CHEN F., *J. Phys. Chem. C*, 113 (2009), 12848.
- [14] GU D.E., YANG B.C., HU Y.D., *Catal. Commun.*, 9 (2008), 1472.
- [15] ZHU W.G., QIU X.F., IANCU V., *Phys. Rev. Lett.*, 103 (2009), 226401.
- [16] SUN R., WANG Z.C., SHIBATA N., IKUHARA Y., *RSC Adv.*, 5 (2015), 18506.
- [17] YANG H.G., SUN C.H., QIAO S.Z., ZOU J., LIU G., SMITH S.C., CHENG H.M., LU G.Q., *Nature*, 453 (2008), 638.
- [18] ZHOU P., WU J.H., YU W.L., ZHAO G.H., FANG G.J., CAO S.W., *Appl. Surf. Sci.*, 319 (2014), 167.
- [19] OH S.M., KIM S.S., LEE J.E., ISHIGAKI T., PARK D.W., *Thin Solid Films*, 435 (2003), 252.
- [20] OZAKI H., IWAMOTO S., INOUE M., *Chem. Lett.*, 34 (2005), 1082.
- [21] YANG K.S., DAI Y., HUANG B.B., *Chem. Phys. Lett.*, 456 (2008), 71.
- [22] SHI W.M., CHEN Q.F., XU Y., WU D., HUO C.F., *Appl. Surf. Sci.*, 257 (2011), 3000.
- [23] YANG X.X., CAO C.D., ERICKSON L., HOHN K., MAGHIRANG R., KLABUNDE K., *Appl. Catal. B-Environ.*, 91 (2009), 657.
- [24] LONG R., ENGLISH N.J., *Chem. Mater.*, 22 (2010), 1616.
- [25] OZAKI H., IWAMOTO S., INOUE M., *Ind. Eng. Chem. Res.*, 47 (2008), 2287.
- [26] ZHANG J.F., ZHOU P., LIU J.J., YU J.G., *Phys. Chem. Chem. Phys.*, 16 (2014), 20382.
- [27] KOHN W., SHAM L.J., *Phys. Rev. A*, 140 (1965), 1133.
- [28] PAYNE M.C., TETER M.P., ALLEN D.C., ARIAS T.A., JOANNOPOULOS J.D., *Rev. Mod. Phys.*, 64 (1992), 1045.
- [29] PERDEW J.P., BURKE K., ERNZERHOF M., *Phys. Rev. Lett.*, 77 (1996), 3865.
- [30] LI H.P., LV S.H., WANG Z.C., XIA Y.J., BAI Y.J., LIU X.J., MENG J., *J. Appl. Phys.*, 111 (2012), 103718.
- [31] LV S.H., LI H.P., WANG Z.C., HAN L., LIU Y., LIU X.J., MENG J., *Appl. Phys. Lett.*, 99 (2011), 202110.
- [32] LONG R., ENGLISH N.J., *Chem. Phys. Lett.*, 478 (2009), 175.
- [33] ZENG W., LIU T.M., WANG Z.C., TSUKIMOTO S., SAITO M., IKUHARA Y., *Mater. Trans.*, 51 (2010), 171.34
- [34] WANG Z.C., SAITO M., MCKENNA K.P., GU L., TSUKIMOTO S., SHLUGER A.L., IKUHARA Y., *Nature*, 479 (2011), 380.
- [35] FAHMI A., MINOT C., SILVI B., CAUSA M., *Phys. Rev. B*, 47 (1993), 11717.

Received 2014-11-04

Accepted 2015-05-19